ACS APPLIED MATERIALS & INTERFACES

Research Article

www.acsami.org

Polysiloxane-Based Block Copolymers with Marine Bacterial Anti-Adhesion Properties

The Hy Duong,[†,‡] Jean-François Briand,[†] André Margaillan,[†] and Christine Bressy*[,†]

[†]Université de Toulon, Laboratoire MAPIEM, EA 4323, 83957 La Garde, France

[‡]The University of Danang, University of Science and Technology, 54 Nguyen Luong Bang, Danang, Vietnam

Supporting Information

ABSTRACT: Di- and triblock copolymers based on *tert*-butyldimethylsilyl methacrylate (MASi) and poly(dimethylsiloxane) (PDMS) macro-RAFT agents were synthesized resulting in copolymers with predictable molar masses and low dispersities ($Đ$ < 1.2). The block copolymers exhibited two glass transition temperatures, corresponding to the PDMS- and poly(*tert*-butyldimethylsilyl methacrylate) (PMASi)-enriched phases, respectively. Contact angle measurements revealed the influence of the copolymer composition on their surface free energy, with block copolymers exhibiting surface free energies as low as 15.0 mJ m^{-2}. A laboratory assay using 96-well plates was used to assess the activity of the block copolymers against two marine bacteria (*Pseudoalteromonas* sp. and *Shewanella* sp.) isolated from the Mediterranean Sea. Coatings based on PDMS-based block copolymers demonstrated anti-adhesive performances against the two strains better than that of the coating containing only PMASi-based polymers. Coatings based on diblock copolymers demonstrated antifouling performances in the field that were better than those of the corresponding coatings containing triblock copolymers. Results of both lab and field assays showed that the antifouling properties were related to coatings possessing the highest receding water contact angle.

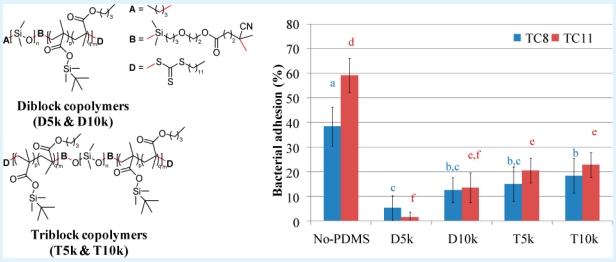

KEYWORDS: *block copolymer, PDMS, bacteria, anti-adhesion, antifouling, receding contact angle*

1. INTRODUCTION

Marine biofouling is an undesired accumulation of micro- and macroorganisms on immersed surfaces that leads to economically and environmentally related negative effects. Marine fouling generates an increase in the drag resistance of a ship moving through water by increasing its surface roughness and consequently increases fuel consumption and emission of greenhouse gases.[1] Technological problems in fluid flow systems, in ocean monitoring equipment for coastal water quality assessment, or in deep-sea sensors[2] have been reported to reduce their operating service life. The process of biofilm formation and biofouling is a multistep process. The initial step of biofilm formation is the colonization of surfaces by bacteria, followed by diverse microorganisms that lead to a complex microbial community.[3] Bacteria and also diatoms secrete matrixes of exopolymeric substances forming highly complex and dynamic three-dimensional (3D) structures. The adhesion of pioneer bacteria, prior to biofilm development, is a process that is controlled by a number of variables, including the surface composition, the structure of the planktonic community, and environmental factors. In addition, there is more and more evidence that macrofouler settlement is controlled at least in part by biofilms.[3] Therefore, bacterial adhesion is probably one of the most critical steps to target using efficient antifouling strategies.

For the marine shipping industries, two main long-lasting and efficient AF coatings are on the market: (i) self-polishing copolymer-based coatings (SPCs), which act on the marine organisms by inhibiting or limiting their settlement using the release of biocides embedded in a polymer matrix, and (ii) nontoxic fouling release coatings (FRCs), which inhibit the settlement of organisms and enhance the easy removal of settled organisms. The former coatings are mainly composed of polymers bearing seawater hydrolyzable side groups leading to the renewal of the coating surface by an erosion process and to the control of the rate of release of biocides.[4,5] Silylester (meth)acrylate, copper acrylate, and zinc acrylate are commonly used as hydrolyzable monomer units.[6] The latter coatings are mainly composed of a poly(dimethylsiloxane) (PDMS) elastomer matrix.[7,8] The fundamental properties of PDMS elastomers are related to the specific characteristics of the siloxane bonds, i.e., the combination of a flexible backbone and low-surface free energy side groups that minimize the adhesion strength between a fouling organism and the substrate, so that the organism can be removed by hydrodynamical stress during navigation or by a simple mechanical cleaning. This specific fouling release property has traditionally been related to the surface hydrophobicity and low energy but is also influenced by other parameters, including the surface

Received: May 15, 2015
Accepted: June 29, 2015
Published: June 29, 2015

© 2015 American Chemical Society

DOI: 10.1021/acsami.5b04234
ACS Appl. Mater. Interfaces 2015, 7, 15578−15586

roughness, the elastic modulus, and the thickness of the film coating.[9]

The aim of this study is the development of hybrid FRC/SPC coatings that are biocide-free and are efficient against the adhesion of pioneer marine bacteria and macroorganisms. Diblock and triblock copolymers combining poly(*tert*-butyldimethylsilyl methacrylate) (PMASi), as a hydrolyzable "SPC-type" block, and PDMS, as a hydrophobic "FRC-type" block, have been synthesized using the RAFT process. The low surface free energy of the polymer films, characteristic of FRC, has been demonstrated using contact angle measurements at the initial stage and after their immersion in artificial seawater for 1 month. Static and dynamic water contact angle values have also been assessed to improve our understanding of the variation of the surface properties of coatings with immersion time. The mass loss of the polymer films, characteristic of SPC coatings, has been assessed by gravimetric investigations during a 6 month immersion test. The anti-adhesion activity of polymer films has been investigated with respect to two marine bacteria isolated from marine biofilms through laboratory tests and macroorganisms through field tests. Scheme S1 of the Supporting Information shows the general scheme of work of this study. Relations between the physicochemical properties of the coating surface and its antifouling activity have been investigated using a multiparameter statistical analysis.

2. EXPERIMENTAL SECTION

2.1. Materials. *tert*-Butyldimethylsilyl methacrylate (MASi) was synthesized as described elsewhere, distilled under reduced pressure, and stored under argon before being used.[10] α-Hydroxyethylpropoxyl-ω-propyl poly(dimethylsiloxane)s (PDMS-OH) of 5000 g mol^{-1} (5k PDMS-OH) and 10000 g mol^{-1} (10k PDMS-OH) and α,ω-dihydroxyethylpropoxyl-PDMS (5k HO-PDMS-OH and 10k HO-PDMS-OH) (Gelest) were used as received. 4-Cyano-4-(dodecylsulfanylthiocarbonyl)sulfanylpentanoic acid (CTA) (Strem Chemicals) was used as received. Dicyclohexylcarbodiimide (DCC), *tert*-butyl(chloro)dimethylsilane, 4-(dimethylamino)pyridine (DMAP), hexane, methanol, acetonitrile, and ethyl acetate were purchased from Sigma-Aldrich and used as received. 2,2′-Azobis(isobutyronitrile) (AIBN) was purchased from Sigma-Aldrich and purified by recrystallization from methanol. Butyl methacrylate (BMA), toluene, and dichloromethane (DCM) were purchased from Sigma-Aldrich and distilled under reduced pressure to remove inhibitors before use. Artificial seawater was prepared in our laboratory (ASTM standard D 1141-90). Diiodomethane (CH_2I_2, Sigma-Aldrich) was used as received.

For bacterial attachment studies, two bacterial strains that belong to the family of γ-proteobacteria, *Pseudoalteromonas lipolytica* (TC8) and *Shewanella pneumatophori* (TC11), were used. TC8 was isolated in February 2008 and TC11 in June 2010 in the Toulon Bay (Mediterranean Sea, France). These two bacterial strains are Gram-negative and classified as hydrophilic bacteria.[11,12]

2.2. Characterization Methods. ^{1}H NMR measurements were taken on a Brüker Advance 400 (400 MHz) spectrometer with deuterated chloroform ($CDCl_3$) as the solvent at room temperature.

The number-average molar mass (M_n) and dispersity ($Đ$) of polymers were determined by triple-detection size exclusion chromatography (TD-SEC). Analyses were performed on a Viscotek apparatus, composed of a GPC Max (comprising a degasser, a pump, and an autosampler) with a TDA-302 (RI refractive index detector, right and low angle light scattering detector at 670 nm, and viscometer), and an ultraviolet (UV) detector (λ = 298 nm). The following columns were used: a Viscotek HHR-H precolumn and two Viscotek ViscoGel GMHHR-H columns. THF was used as the eluent with a flow rate of 1.0 mL min^{-1} at 30 °C. For each precipitated polymer, the refractive index increment (dn/dc) was determined using the OmniSec software, from a solution with a known concentration (~10 mg mL^{-1}) filtered through a 0.2 mm PTFE filter.

Differential scanning calorimetric (DSC) measurements were performed on a DSC Q10 apparatus from TA Instruments calibrated with indium. Polymer samples weighing 15−20 mg were run at equal heating and cooling rates, 10 °C min^{-1}, under a constant stream of nitrogen. The polymer samples were first scanned from room temperature to 100 °C and then cooled to −165 °C. The samples were held at −165 °C for 5 min to allow the system to attain thermal equilibrium before the second heating scan. The first heating ramp of each sample was discarded for this work. The glass transition temperature (T_g) values were determined as the midpoint between the onset and the end of a step transition using the TA Instruments Universal Analysis 2000 software. The melting and crystallization temperatures were recorded at the maximal value of the endothermic and exothermic peaks, respectively.

The atomic force microscopy (AFM) images were obtained on a Multimode AFM V instrument (Veeco, Bruker AXS) in tapping mode. Silicon tips used were of the RTESP (BRUKER) type whose spring constant is between 20 and 80 N/m with a resonance frequency of ~380 kHz. The AFM images have been recorded with a 1/0.5 ratio.

2.3. Synthesis of Macro-Chain Transfer Agents (macro-RAFT agents) and Block Copolymers. In our previous publication, we reported the conditions and procedures used for the synthesis of monofunctional macro-RAFT agents.[13] A similar protocol was used for the synthesis of difunctional macro-RAFT agents. In brief, the molar ratio of reactive agents is 1:1.5:2:0.2 ([OH]:[COOH]:[DCC]:[DMAP]), and with a molar concentration of the hydroxyl group equal to 28 mmol L^{-1}, the reaction time and temperature are 15 h and 40 °C, respectively. The reaction mixture was then cooled in the freezer and filtered to remove any solid impurities. The solvent was removed under reduced pressure. Hexane was added, and the resulting solution was treated with methanol, a saturated NaCl solution, and then deionized water. Magnesium sulfate was used to dry the product. Finally, the product was passed through a silica gel column with a hexane/ethyl acetate mixture as the eluent. A final pale yellow liquid product was obtained by drying under vacuum. The macro-RAFT agents are listed in Table 1.

Table 1. Short Names of Macro-RAFT Agents

type of PDMS precursor	molar mass of PDMS precursor (^{1}H NMR) (g mol^{-1})	name of macro-RAFT agent
PDMS-OH	5100	5k monofunctional macro-RAFT agent
	10800	10k monofunctional macro-RAFT agent
HO-PDMS-OH	4550	5k difunctional macro-RAFT agent
	10100	10k difunctional macro-RAFT agent

PDMS-*block*-P(MASi-*stat*-BMA) and P(MASi-*stat*-BMA)-*block*-PDMS-*block*-P(MASi-*stat*-BMA) copolymers with target M_n values were synthesized using the macro-RAFT agents reported in Table 1. The macro-RAFT agent concentration was estimated from eq 1 for a given M_n value assuming that the termination event is negligible and that all polymer chains bear one CTA end group. $M_{n,target}$ is defined at 100% of monomer conversion.[14]

$$M_n = \frac{[M]_0 M_{monomer}}{[CTA]_0 + df[I]_0(1 - e^{-k_d t})} \times \rho + M_{CTA} \quad (1)$$

where $[M]_0$, $[CTA]_0$, and $[I]_0$ are the initial concentrations of monomer, macro-RAFT agent, and initiator, respectively, $M_{monomer}$ is the molar mass of the monomer, ρ is the fractional conversion, k_d is the rate constant for initiator dissociation, f is the initiator efficiency factor, d is the number of chains produced from radical−radical reaction, and M_{CTA} is the molar mass of the macro-RAFT agent.

DOI: 10.1021/acsami.5b04234
ACS Appl. Mater. Interfaces 2015, 7, 15578−15586

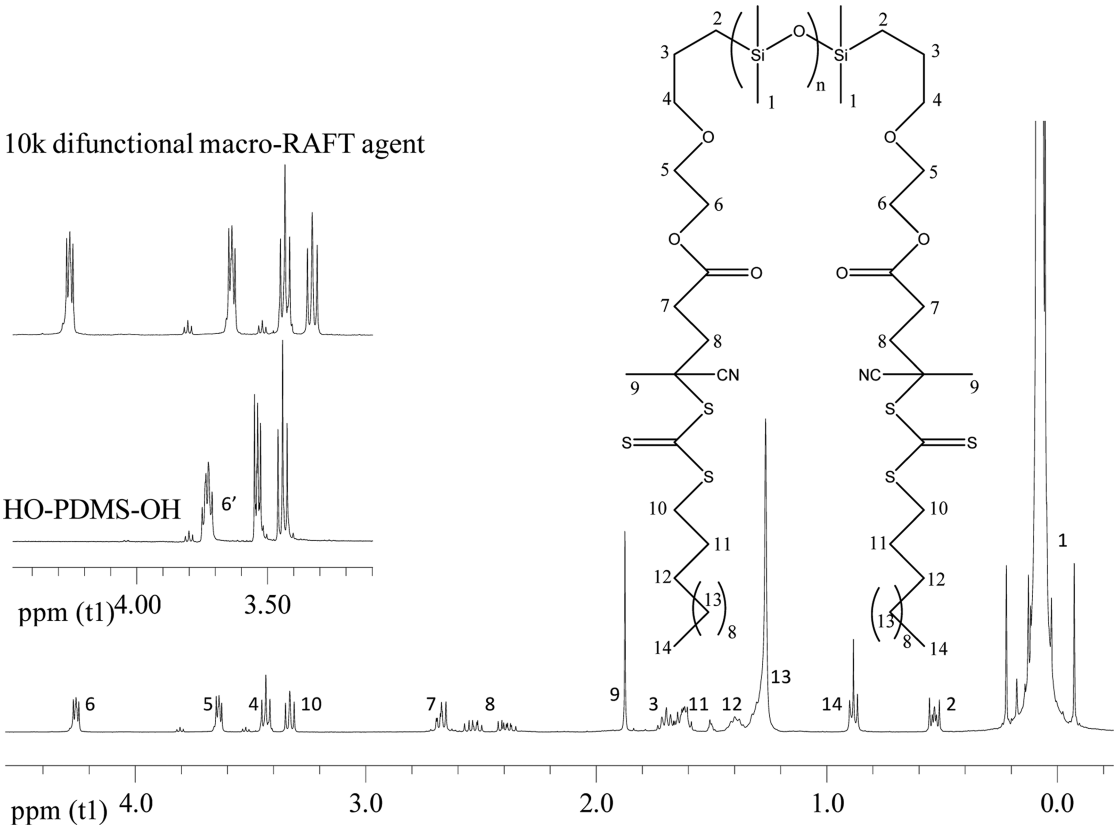

Figure 1. ^{1}H NMR spectrum of the 10k difunctional macro-RAFT agent.

The monomer concentration and the molar ratios of macro-RAFT agent to AIBN and BMA to MASi in toluene were fixed to 1.5 M, 5, and 6, respectively. The polymerization procedure was described elsewhere.[13] Dried powders were obtained by precipitating the copolymers in methanol and dried at 40 °C, under vacuum to a constant weight.

The abbreviations used for samples are as follows: D5k and D10k for PDMS-based diblock copolymers with PDMS molar masses of 5 kg mol^{-1} and 10 kg mol^{-1}, respectively, and T5k and T10k for PDMS-based triblock copolymers with PDMS molar masses of 5 kg mol^{-1} and 10 kg mol^{-1}, respectively. The polymer sample without PDMS block is called "No-PDMS".

2.4. Coating Preparation. Each polymer was dissolved in toluene, at a solid content of 40−50 wt %, and applied on abraded poly(vinyl chloride) (PVC) substrates with a bar-coater, resulting in ∼100 μm dried thickness coatings. The surfaces of the samples used for the contact angle measurements (also for the erosion test) and for *in situ* seawater immersion tests were 25 mm × 45 mm and 50 mm × 50 mm, respectively. The coated plates were left to dry in the open air for 15 days.

2.5. Contact Angle Measurement. Static contact angle measurements were taken at room temperature using a sessile drop method with a DIGIDROP contact angle meter from GBX Instruments. Two test liquids, deionized water and diiodomethane, were used. The liquid drop volumes were 1 and 0.5 μL for water and diiodomethane, respectively. The reported contact angles were an average of five individual measurements in different regions of the same coating. The surface free energy of the coatings (γ_s) and its dispersive (γ_s^D) and polar (γ_s^P) components were calculated using the Owens−Wendt method.[15] Dynamic contact angle measurements were taken under ambient conditions by using the dynamic sessile drop technique. A water drop is growing on a syringe tip and is picked up by the surface. The water was inflated and sucked up from the surface, and the advancing and receding angles were obtained. The syringe tip never leaves the liquid drop.

2.6. Erosion. The hydrolytic degradation testing was conducted in ASW at 25 °C. The polymer film coated on a PVC foil (25 mm × 45 mm) was prepared via a solution-casting method, as reported before. The weighted sample of each dried coating together with its foil was incubated in a tank of ASW that was changed every 2 weeks. At a predetermined time, the sample was taken out, rinsed three times with deionized water, and left to dry in the open air overnight. The mass loss (weight percent) was estimated from eq 2:

$$\text{mass loss}\ (\%) = \frac{w_0 - w_t}{w_0 - w_{\text{foil}}} \times 100 \qquad (2)$$

where w_0, w_t, and w_{foil} are the initial weight of the foil coated with polymers, the weight of the coated foil at time t, and the weight of the foil without a coating, respectively. For each sample, three coated foils were prepared and measured, and data points were averaged.

2.7. Bacterial Attachment Studies. Bioassays were performed in black 96-well flat-bottom microplates in polypropylene (PP). Thirty microliters of each polymer solution, at a solid content of 40−50 wt %, was added to the eight wells of the same column. The microplates were left to dry in the open air for 15 days. Then they were washed three times with deionized water and allowed to stir for 2 h. The water was then removed, and microplates were dried for 10 min. Finally, they were sterilized under UV light for 30 min. The bacteria were cultured in Vaatanen nine-salt solution (VNSS) at 20 °C and stirred at 120 rpm, recovered early in the stationary phase, and then centrifuged for 10 min at 6000 rpm. The culture medium was removed and replaced with artificial seawater (ASW, Sigma-Aldrich). Six over eight wells of the microplates' columns were then seeded at an optical density (OD_{600}) of 0.25 for both TC8 and TC11. The completion of the bioassay requires knowledge of the optimal phase of accession, the seed time, and the seed density. The parameters are derived from previous work in the laboratory.[12] To enhance their ability to adhere, the bacteria were seeded in the stationary phase into a carbon-free medium (ASW). After an optimal adhesion time of 15 h, the nonadherent bacteria were removed from the microplate. Three

DOI: 10.1021/acsami.5b04234
ACS Appl. Mater. Interfaces 2015, 7, 15578−15586

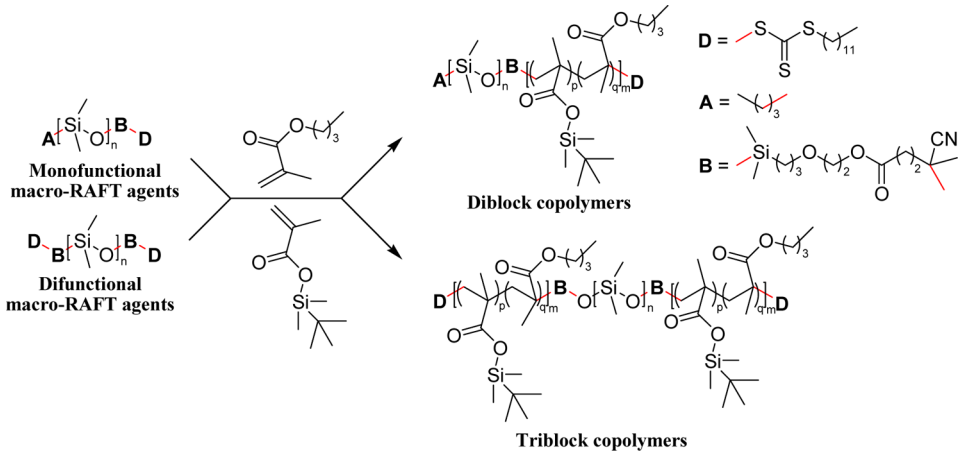

Figure 2. General synthetic pathway of di- and triblock copolymers.

Table 2. Characteristics of Copolymers

			M_n (g mol^{-1})				T_g (°C)			
	polymer	$\%_{mass}$ DMS/MASi/BMA	target	meth. block[a]	TD-SEC	$Đ$	T_{g1}	T_{g2}	T_m (°C)	ΔH (J g^{-1})
	No-PDMS	0/18/82	9100		11100	1.13	–	31	–	–
diblock	D5K	39/11/50	15400	8600	16800	1.12	−126	29	–	–
	D10K	57/8/35	20000	8100	23600	1.04	−124	32	−40	12
triblock	T5K	37/12/51	15100	4400	18600	1.10	−128	16	–	–
	T10K	56/9/35	20200	4500	21400	1.07	−125	14	−50	3.5

[a] M_n of the methacrylic block determined by ^{1}H NMR.

successive washings with NaCl (36 g L^{-1}) were performed; 200 μL of crystal violet (CV) (0.1%) was added to the wells. The incubation lasts 30 min, and the dye was then removed. Three successive washings were performed with 200 μL of NaCl (36 g L^{-1}). Finally, the CV was extracted with 200 μL of 50% ethanol for 15 min. The extraction solution was then measured at 595 nm. A relative rate of adhesion to PS was calculated for each well from the following equation (eq 3):

$$\text{adhesion}\ (\%) = \frac{(\text{OD}_{\text{with bacteria}} - \text{OD}_{\text{blank}})_{\text{coating}}}{(\text{OD}_{\text{with bacteria}} - \text{OD}_{\text{blank}})_{\text{PScontrol}}} \times 100 \quad (3)$$

where $\text{OD}_{\text{with bacteria}}$ is the optical density of the CV solution extracted from inoculated wells with bacteria and OD_{blank} is the optical density of the CV solution extracted from wells without bacteria.

2.8. Antifouling Field Studies. *In situ* seawater immersions were conducted in the Toulon Bay in a semienclosed pond of the military harbor (43°06′25″N, 5°55′41″E), which is the current immersion site for the assessment of antifouling paints for the MAPIEM laboratory. The plates are placed on racks and immersed in 1−1.4 m of water. Each coating is immersed in duplicate. A blank sand-blasted PVC plate is also immersed. At every inspection, the plates are rinsed with a water jet and photographed and a detailed inspection of the plates is achieved. This light rinsing procedure removes slime and hinders inspection. All the samples were immersed on May 14, 2013.

A French practice adapted from French standard NF T 34-552 was used to assess the AF efficacy of coatings. This standard requires that we report (i) the type of macrofoulers attached to the surface and (ii) the estimated percentage of the surface covered by each type of macrofouler (intensity factor, i.e., IF). The inspection was performed 1 cm from the edges of the panel. An efficacy parameter N was defined as follows: $N = \sum(\text{IF} \times \text{SF})$, where SF is defined as a severity factor, which takes into account the frictional drag penalty of ship hulls that can be attributed to increased surface roughness due to foulers.[16]

2.9. Statistical Analysis. Two-dimensional analysis of variance (2D-ANOVA) was performed to highlight the significance of differences observed in the adhesion of marine bacteria but also contact angles using GraphPad Prism5.

A principal component analysis (PCA) was used to analyze macrofouler communities colonizing immersed surfaces quantitatively and qualitatively (XLSTAT).

3. RESULTS AND DISCUSSION

3.1. Synthesis of Macro-RAFT Agents and Block Copolymers. Mono- and difunctional macro-RAFT agents were synthesized quantitatively from hydroxylated PDMS and CTA by esterification. The quantitative conversion of this reaction was confirmed by ^{1}H NMR (Figure 1). The signal of the methylene protons adjacent to the hydroxyl group of the PDMS precursor at 3.73 ppm disappeared from the spectrum of the products of reaction.

The synthesis of di- and triblock copolymers was conducted in the presence of mono- and difunctional macro-RAFT agents, respectively (Figure 2). The theoretical M_n values of the methacrylic block in the diblock and triblock copolymers are 10000 and 5000 g mol^{-1}, respectively. Because of the high glass transition temperature (T_g) of PMASi, butyl methacrylate was used as a co-monomer to obtain continuous films with no cracks. The control of the polymerization of MASi and BMA on the macro-RAFT agent chains was previously demonstrated by the first-order kinetic of monomer consumption together with a linear increase in the M_n value with monomer conversion.[13] ^{1}H NMR spectra of di- and triblock copolymers are presented in Figures S1 and S2 of the Supporting Information.

Table 2 shows that the copolymers containing a weight content of PDMS higher than 37% exhibit two T_g values. The lower T_g value is the T_g of the PDMS block.[13] The higher T_g value corresponds to the T_g of the methacrylic-based block of the two diblock copolymers (D5K and D10K). In addition, the T_g value of the PMASi-based blocks in triblock copolymers (T5K and T10K) corresponds to half the T_g of the PMASi-based blocks in diblock copolymers as the length of these

DOI: 10.1021/acsami.5b04234
ACS Appl. Mater. Interfaces 2015, 7, 15578−15586

Table 3. Static Contact Angles and Surface Free Energies of Polymer Films

		static contact angle (deg)		surface free energy (mJ m^{-2})		
	polymer (wt % DMS)	θ_{H_2O}	$\theta_{CH_2I_2}$	γ_s	γ_s^D	γ_s^P
	No-PDMS (0)	88.6 ± 2	63.5 ± 2.4	27.6	23.3	4.3
diblock	D5K (39)	100.5 ± 1	53.6 ± 1.2	32.9	32.7	0.2
	D10K (57)	108.3 ± 1	92.2 ± 2	12.2	10.2	2.0
triblock	T5K (37)	101.7 ± 1.2	63.8 ± 1.8	26.5	26.0	0.5
	T10K (56)	105.6 ± 1.6	86.6 ± 7.2[a]	14.6	12.7	1.9

[a]The high standard deviation value for the CH_2I_2 contact angle is due to the interaction between the CH_2I_2 and the film surface, seen by residual traces of the liquid droplet at the surface after evaporation.

blocks is divided by 2. These results demonstrate that the PDMS- and PMASi-based blocks are immiscible. D10K (diblock copolymer) and T10K (triblock copolymer) based on 10k PDMS showed melting points at −40 and −50 °C, respectively. This melting point corresponds to the melting of PDMS chains that crystallize during the first cooling and the second heating step (cold crystallization) of the DSC analysis. The values of the melting enthalpy demonstrated that the crystallinity in T10K was less than in D10K (12 J g^{-1} for D10K and 3.5 J g^{-1} for T10K). This could be explained by the lower mobility of the PDMS chain in T10K that was anchored by methacrylic blocks at both chain ends. No crystallization of PDMS chains was observed in the 5k PDMS diblock (D5K) and triblock (T5K) copolymers. This result could be explained by the low PDMS content of polymers or the shorter PDMS chains in comparison to the one in D10K and T10K copolymers.

3.2. Erosion of Coatings. Hydrolysis of silylester groups in polymer chains during immersion in ASW results in the presence of more hydrophilic groups (COO^-) on the polymer chains.[17] If the quantity of hydrophilic groups is sufficiently large, the polymer chain could become soluble, so erosion could occur. A work of Lejars et al.[18] showed that graft copolymers of MASi and poly(dimethylsiloxane) methacrylate (PDMS-MA) containing ∼50% MASi in mass swelled in the initial stage and slightly eroded after immersion for 1 or 2 months. In this study, butyl methacrylate was used as co-monomer to obtain continuous films with no cracks. As a result, the hydrolyzable MASi content in polymers was very low (from 8 to 18% in mass) in comparison with that of the copolymers reported in the work of Lejars et al. It is shown that there was initially a swelling followed by a very slight erosion (<0.2% of mass loss) after immersion for 1 month for the diblock copolymers and after immersion for 2 months for the triblock copolymers and the PDMS-free copolymer (No-PDMS).

3.3. Wettability of Coatings. *3.3.1. Static Contact Angle and Surface Free Energy.* Static water and diiodomethane contact angles and surface free energies of coatings are listed in Table 3. Water contact angles are shown to increase with an increasing PDMS content in the block copolymers. The increase in the hydrophobic character of the polymer film surfaces could be explained by a high density of dimethylsiloxane groups at the surface. Two polymers with the highest PDMS content, D10K and T10K, also exhibit diiodomethane contact angle values close to 90° together with the lowest surface free energy values (<20 mJ m^{-2}).

Figure 3 shows that the high water contact angle values of polymer films are maintained during immersion in ASW, except for a slight decrease for No-PDMS that does not contain any PDMS.

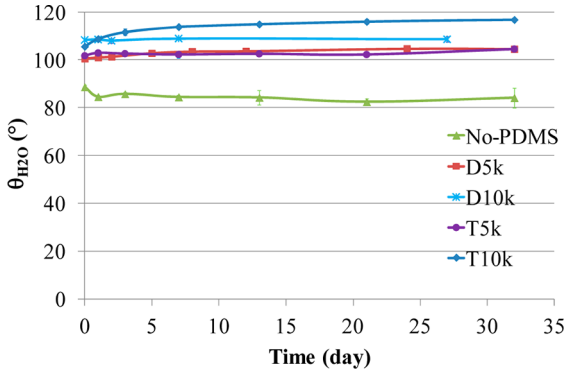

Figure 3. Evolution of the static water contact angle with ASW immersion time.

3.3.2. Dynamic Contact Angle. Figure 4 shows variations in the water advancing contact angle (θ_{adv}) and the water receding

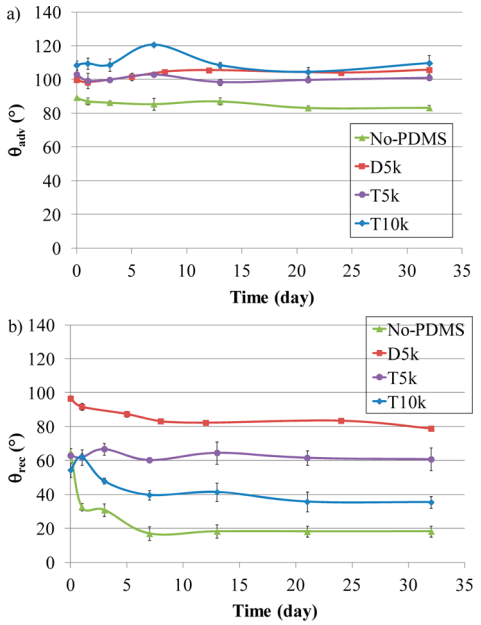

Figure 4. Evolution of (a) the advancing water contact angle and (b) the receding water contact angle of the coatings with ASW immersion time.

contact angle (θ_{rec}) during immersion of polymer films in ASW. θ_{adv} is a measure of the hydrophobic character of the surface, while θ_{rec} is a measure of the hydrophilic character of the surface. The values of θ_{adv} were relatively stable and close to the values of the static contact angles. In contrast, θ_{rec} decreased after a short period of immersion (24 h) and became stable

DOI: 10.1021/acsami.5b04234
ACS Appl. Mater. Interfaces 2015, 7, 15578−15586

(except for T5K-based coating). The order of magnitude of θ_{rec} between the polymers became constant after immersion for 24 h, and the threshold of θ_{rec} of each polymer was reached after 7 days. This decrease in θ_{rec} during immersion might be explained by a variation in the chemical composition of the surface coming from the hydrolysis of silylester groups[19] within the copolymers and/or a reorganization of the surface leading to a higher ratio of PMASi to PDMS. Then, the amount of the resulting polar groups increased. No-PDMS-based coating exhibits a greater decrease in θ_{rec} as it contains no PDMS block. The concentration of hydrolyzable MASi units at the surface was therefore the highest. In PDMS-based copolymers, because the surface free energy of PDMS chains (i.e., 19.9 mJ m^{-2})[20] is lower than that of methacrylic chains, the DMS groups preferentially segregate at the air−polymer interface.[21] This phenomenon occurs during the drying step. As a consequence, the concentration of hydrophilic groups at the surface decreases and θ_{rec} increases. The highest value of θ_{rec} of the 5k PDMS-based diblock copolymer (D5K) means that its surface was richest in PDMS. Nevertheless, the θ_{rec} of the 5k PDMS-based triblock copolymer (T5K) was lower than that of the diblock copolymer (D5K) even if it exhibits a similar PDMS content. This result could come from the difficulty in migration of PDMS chains from the bulk to the surface because of their anchoring to methacrylic blocks at both ends. The PDMS content in the 10k PDMS-based triblock copolymer (T10K) was also much higher than in the 5k PDMS triblock copolymer (T5K), but the value of θ_{rec} was ∼20° lower. A first investigation by AFM showed the difference in the distribution of PDMS and methacrylic phases at the surface between these two samples (Figure 5). There was a homogeneous phase distribution at the surface of T5K, while spherical domains were observed at the surface of the T10K coating. This means that PDMS components covered predominantly the surface of the T5K-based coating, making it hydrophobic with a weak variation in θ_{rec} with immersion time. For the T10K-based coating, the observed large domains reveal a nonhomogeneous surface with the juxtaposition of PDMS and methacrylic phases at the surface. On the surface of the methacrylic phase, there was less or no PDMS. As a consequence, this phase leads to a more hydrophilic surface with stronger interaction with water in comparison with the surface of T5k-based coating. This polar interaction results in a greater decrease in θ_{rec}. Nevertheless, the presence of hydrophobic PDMS phases on the surface of the T10k-based coating keeps θ_{rec} at a high value. Because θ_{rec} is more sensible for the hydrophilic character of the surface, a greater variation in θ_{rec} with immersion time was observed on the T10k-based coating in comparison with that of the T5k-based coating. The absence of domains on the surface of the D5K-based coating was also observed as the corresponding triblock T5K coating, resulting in high values of θ_{rec} with immersion time. Unfortunately, it was not possible to perform either dynamic contact angle measurements or AFM for the 10k PDMS-based diblock copolymer (D10K) because of the waviness of its surface.

It is thus worth noting that the assessment of the receding contact angle is more appropriate to show any reorganization or chemical heterogeneity at the surface during immersion. The static water contact angle does not reflect any change in the hydrophilic character of the tested surfaces.

3.4. Bacterial Anti-Adhesion Studies. Figure 6 shows that the PDMS-free coating (No-PDMS) is significantly less efficient than the four PDMS-based coatings ($p < 0.001$). In addition, the only difference between the two strains was observed for the No-PDMS-based coating, which is more efficient against the adhesion of TC8. All PDMS-based coatings inhibit the adhesion of the two bacterial strains. The diblock D5K coating with 39 wt % PDMS is more efficient than the three other PDMS-based coatings ($p < 0.0001$). Therefore, we could conclude that the adhesion of the two hydrophilic TC8 and TC11 bacteria is favored on hydrophilic surfaces, i.e., on surfaces with a θ_{H_2O} or θ_{adv} of <90°. This is consistent with the results reported by Bakker et al., who demonstrated that the more hydrophilic bacteria adhered preferentially to the more

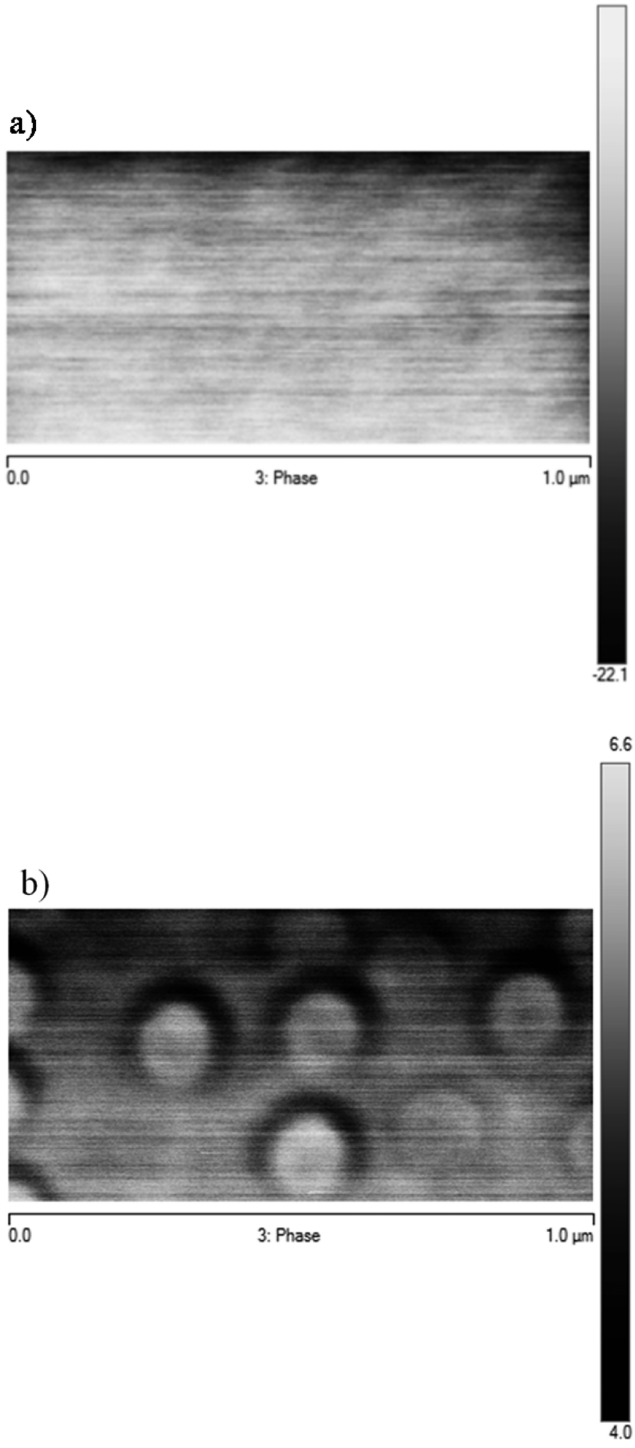

Figure 5. AFM phase images of (a) T5K and (b) T10K films.

DOI: 10.1021/acsami.5b04234
ACS Appl. Mater. Interfaces 2015, 7, 15578−15586

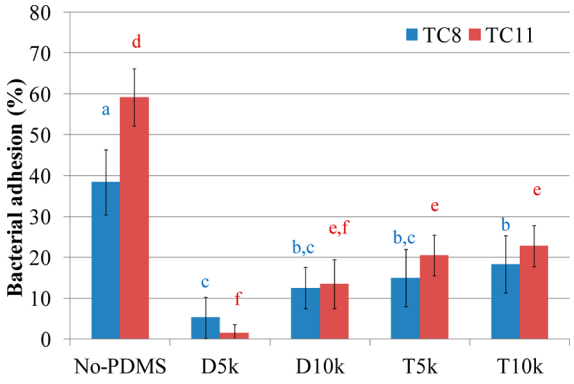

Figure 6. Bacterial adhesion on coatings in 96-well plates using crystal violet. Each coating was tested in six replicates, and the control surface is polystyrene. Standard deviation ± σ. Tukey post hoc tests are presented (2D-ANOVA). Average adhesion values that do not share a letter are significantly different.

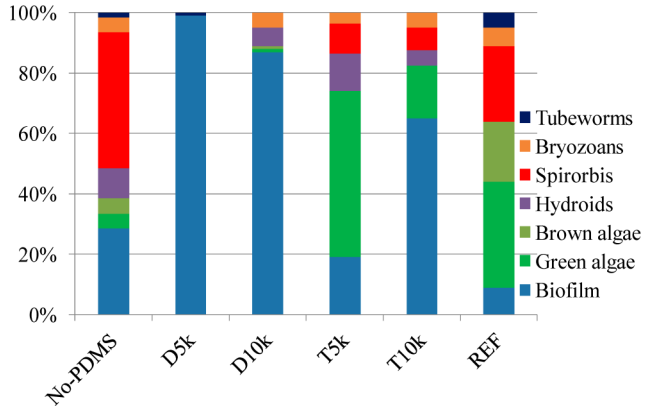

Figure 7. Relative diversity of marine organisms on coating surfaces after immersion for 2 months in Toulon Bay.

hydrophilic substrates and vice versa.[22] This observation was also claimed by Ista et al., who showed that the number of hydrophobic bacteria attached to the substrate increases with an increase in the hydrophobic character of the substrate.[23] As shown in Figure 4b, the surface properties of most of the coatings changed with immersion time. There was a sharp decrease in the θ_{rec} value of the No-PDMS-based coating, while the θ_{rec} value of the D5K-based coating remained at the highest value. The adhesion of bacteria could be affected by these variations over time. It is worth noting that the bacterial adhesion of TC8 and TC11 correlates statistically with the values of θ_{rec} obtained after ASW immersion for 24 h, corresponding to the incubation time (for TC11, $n = 4$, $R^2 = 0.953$, and $p < 0.05$; for TC8, $n = 4$, $R^2 = 0.942$, and $p < 0.05$). No correlations were observed between the bacterial adhesion of TC8 and TC11 with the values of θ_{rec} at the initial stage and after ASW immersion for 32 days. As previously reported by Hahnel et al.,[24] we did not show any significant relationship between the surface free energy and bacterial adhesion. Further investigations on a higher number of coatings could be done to confirm the correlation we observed between $\theta_{rec,24\ h}$ and bacterial adhesion.

3.5. Antifouling Field Study. To go further with respect to their antifouling efficacy, the coatings were immersed in natural seawater in Toulon Bay. Table 4 shows that two diblock copolymers (D5K and D10K) and one triblock copolymer (T10K) are the most efficient coatings after immersion for 2 months. It is clearly seen that D5K exhibits the higher antifouling efficacy, i.e., the lowest value of *N*. In addition, there was only 1% of its surface covered by tubeworms; 99% of its surface was covered by a biofilm formed after a short period of immersion (Figure 7). The 10k PDMS-based D10K diblock copolymer is less efficient than the 5k PDMS-based D5K diblock copolymer with 13% of its surface covered by macrofoulers such as hydroids (6%), bryozoans (5%), green algae (1%), and brown algae (1%). The antifouling activity of the 10k PDMS-based T10K triblock copolymer against macrofoulers is better than that of the 5k PDMS-based T5K triblock copolymer because of a lower surface coverage value obtained for hydroids and green algae. The diversity of marine macrofoulers is higher for the PDMS-free coating (No-PDMS). This latter coating is rapidly colonized by bryozoans, spirorbis, green and brown algae, and tubeworms.

Although the antifouling efficacy *N* of the coatings did not correlate with the value of $\theta_{rec,24\ h}$, the coating exhibiting the highest value of θ_{rec} (D5K) showed the best antifouling efficacy in the field. Pictures in Table 5 clearly show that the antifouling activity of the coating based on diblock copolymers (D5K and D10K) is higher than that of the coating based on triblock copolymers (T5K and T10K). It should be noted that the

Table 4. Values of Efficacy Parameter *N* of Coatings after *in Situ* Immersion for 2 Months

	No-PDMS	D5K	D10K	T5K	T10K	ref
N	34	11	18	33	18	30

Table 5. Pictures of Coatings (after light rising) after Immersion for 2 and 7 Months in Toulon Bay

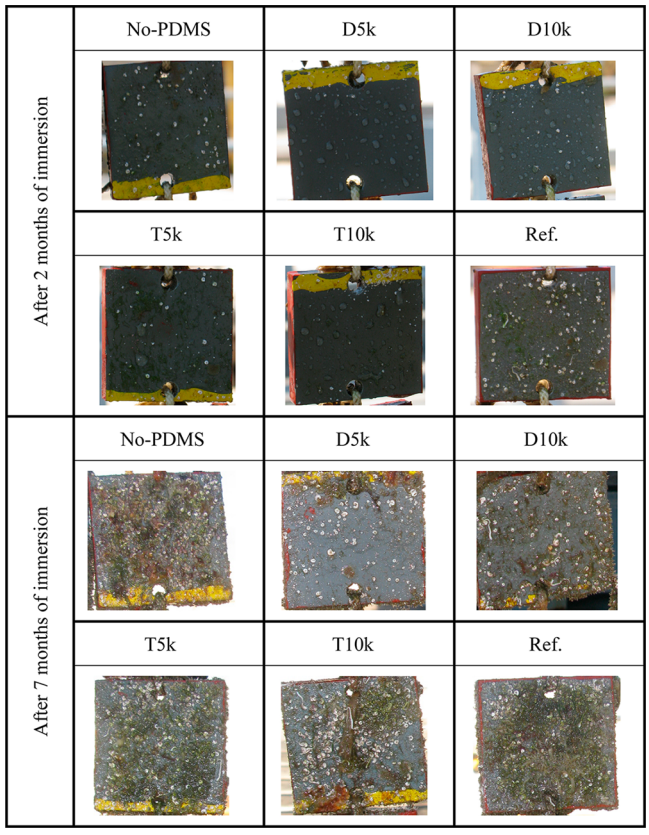

DOI: 10.1021/acsami.5b04234
ACS Appl. Mater. Interfaces 2015, 7, 15578−15586

weight percent of DMS in D5K and T5K is similar. This is also true for D10K and T10K as triblock copolymers.

Figures 7 and 8 show that No-PDMS and to a lesser extent T5K exhibit similarities in macrofouler communities compared

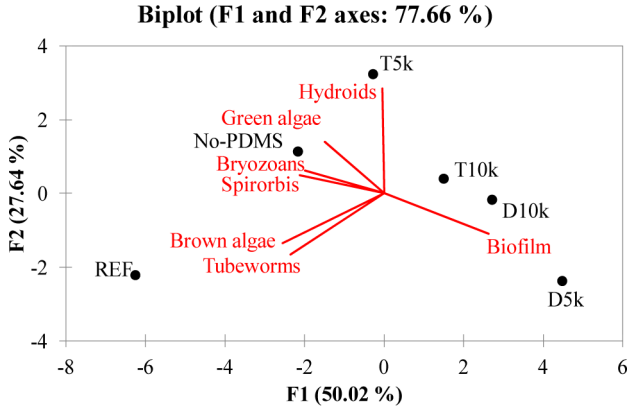

Figure 8. PCA of the macrofouler communities colonizing the immersed surfaces after 2 months in Toulon Bay. The biplot allows the representation of both the observations and the variables on the same graph.

to the uncoated PVC reference, mainly characterized by a high diversity and the dominance of Spirorbis. T5K displays a shift in the colonizing communities with an increasing proportion of nonencrusting organisms (green algae and hydroids). The PCA shows clearly that fouling communities tend to be dominated by biofilms when analyzing T10K, D10K, and D5K. The latter is covered by only a biofilm, which is a clear indication of a maintained high efficacy after immersion for 2 months.

Globally, the marine biofouling communities colonizing PDMS-free and PDMS-based coatings are mainly different from the reference PVC panel, and the adjunction of PDMS in copolymers limits the settlement of macroorganisms (Table 4).

The better antifouling performance of the coating based on the 5k PDMS diblock copolymer D5K is still observed until immersion for 7 months (Table 5). However, the antifouling performance after immersion for 7 months shows that the D5k copolymer is not as satisfying as requested for long-term efficient coatings.

4. CONCLUSIONS

The synthesis of PMASi- and PDMS-based di- and triblock copolymers was effectively controlled by RAFT polymerization, using PDMS macro-RAFT agents with different molar masses. Block copolymers with controlled molar masses and low dispersity were obtained. Because these block copolymers exhibit two distinct T_g values on DSC curves, microphase separations can occur between blocks. The presence of PDMS chains in copolymers was shown to decrease the surface free energy of the resulting coatings. In addition, coatings prepared from these polymers maintained the hydrophobic character of their surface during immersion in artificial seawater. The coating exhibiting the highest receding water contact angle showed the best bacterial anti-adhesion properties and the best field antifouling activity. *In situ* antifouling properties were shown to be enhanced by the adjunction of PDMS in the copolymer and to be affected by the polymer microstructure. Further investigations will be conducted to fully understand the effect of the microstructure on the morphology of the self-assembling polymer chains at the surface of the coating.

■ ASSOCIATED CONTENT

Supporting Information

General scheme of the work (Scheme S1), ^{1}H NMR spectrum of the D5k diblock copolymer (Figure S1), and the ^{1}H NMR spectrum of the T5k triblock copolymer (Figure S2). The Supporting Information is available free of charge on the ACS Publications website at DOI: 10.1021/acsami.5b04234.

■ AUTHOR INFORMATION

Corresponding Author

*E-mail: christine.bressy@univ-tln.fr.

Author Contributions

T.H.D. and J.-F.B. contributed equally to this work.

Notes

The authors declare no competing financial interest.

■ ACKNOWLEDGMENTS

We acknowledge the Vietnamese government for financial support of this research. We thank Brigitte Tanguy for her help in performing laboratory bioassays and Dr. Lénaïk Belec for her contribution to AFM investigations.

■ REFERENCES

(1) Schultz, M. P.; Bendick, J. A.; Holm, E. R.; Hertel, W. M. Economic Impact of Biofouling on a Naval Surface Ship. *Biofouling* **2011**, *27* (1), 87−98.

(2) Delauney, L.; Compère, C.; Lehaitre, M. Biofouling Protection for Marine Environmental Sensors. *Ocean Sci.* **2010**, *6* (2), 503−511.

(3) Salta, M.; Wharton, J. A.; Blache, Y.; Stokes, K. R.; Briand, J.-F. Marine Biofilms on Artificial Surfaces: Structure and Dynamics. *Environ. Microbiol.* **2013**, *15* (11), 2879−2893.

(4) Almeida, E.; Diamantino, T. C.; de Sousa, O. Marine Paints: The Particular Case of Antifouling Paints. *Prog. Org. Coat.* **2007**, *59* (1), 2−20.

(5) Bressy, C.; Hellio, C.; Nguyen, M. N.; Tanguy, B.; Maréchal, J.-P.; Margaillan, A. Optimized Silyl Ester Diblock Methacrylic Copolymers: A New Class of Binders for Chemically Active Antifouling Coatings. *Prog. Org. Coat.* **2014**, *77* (3), 665−673.

(6) Yebra, D. M.; Kiil, S.; Dam-Johansen, K. Antifouling Technology—past, Present and Future Steps towards Efficient and Environmentally Friendly Antifouling Coatings. *Prog. Org. Coat.* **2004**, *50* (2), 75−104.

(7) Choi, S.; Jepperson, J.; Jarabek, L.; Thomas, J.; Chisholm, B.; Boudjouk, P. Novel Approach to Anti-Fouling and Fouling-Release Marine Coatings Based on Dual-Functional Siloxanes. *Macromol. Symp.* **2007**, *249*−*250* (1), 660−667.

(8) Berglin, M.; Wynne, K. J.; Gatenholm, P. Fouling-Release Coatings Prepared from A,ω-Dihydroxypoly(dimethylsiloxane) Cross-Linked with (heptadecafluoro-1,1,2,2-Tetrahydrodecyl)triethoxysilane. *J. Colloid Interface Sci.* **2003**, *257* (2), 383−391.

(9) Lejars, M.; Margaillan, A.; Bressy, C. Fouling Release Coatings: A Nontoxic Alternative to Biocidal Antifouling Coatings. *Chem. Rev.* **2012**, *112* (8), 4347−4390.

(10) Nguyen, M. N.; Bressy, C.; Margaillan, A. Controlled Radical Polymerization of a Trialkylsilyl Methacrylate by Reversible Addition−fragmentation Chain Transfer Polymerization. *J. Polym. Sci., Part A: Polym. Chem.* **2005**, *43* (22), 5680−5689.

(11) Brian-Jaisson, F.; Ortalo-Magné, A.; Guentas-Dombrowsky, L.; Armougom, F.; Blache, Y.; Molmeret, M. Identification of Bacterial Strains Isolated from the Mediterranean Sea Exhibiting Different Abilities of Biofilm Formation. *Microb. Ecol.* **2014**, *68* (1), 94−110.

(12) Camps, M.; Briand, J.-F.; Guentas-Dombrowsky, L.; Culioli, G.; Bazire, A.; Blache, Y. Antifouling Activity of Commercial Biocides vs.

DOI: 10.1021/acsami.5b04234
ACS Appl. Mater. Interfaces 2015, 7, 15578−15586

Natural and Natural-Derived Products Assessed by Marine Bacteria Adhesion Bioassay. *Mar. Pollut. Bull.* **2011**, *62* (5), 1032−1040.
(13) Duong, T. H.; Bressy, C.; Margaillan, A. Well-Defined Diblock Copolymers of Poly(tert-Butyldimethylsilyl Methacrylate) and Poly-(dimethylsiloxane) Synthesized by RAFT Polymerization. *Polymer* **2014**, *55* (1), 39−47.
(14) Keddie, D. J. A Guide to the Synthesis of Block Copolymers Using Reversible-Addition Fragmentation Chain Transfer (RAFT) Polymerization. *Chem. Soc. Rev.* **2014**, *43* (2), 496−505.
(15) Owens, D. K.; Wendt, R. C. Estimation of the Surface Free Energy of Polymers. *J. Appl. Polym. Sci.* **1969**, *13* (8), 1741−1747.
(16) Bressy, C.; Briand, J.-F.; Compère, C.; Réhel, K. Efficacy Testing of Biocides and Biocidal Coatings. In *Biofouling Methods*; Dobretsov, S., Thomason, J. C., Williams, D. N., Eds.; John Wiley & Sons, Ltd.: New York, 2014; pp 332−345.
(17) Xie, L.; Hong, F.; He, C.; Ma, C.; Liu, J.; Zhang, G.; Wu, C. Coatings with a Self-Generating Hydrogel Surface for Antifouling. *Polymer* **2011**, *52* (17), 3738−3744.
(18) Lejars, M.; Margaillan, A.; Bressy, C. Well-Defined Graft Copolymers of Tert-Butyldimethylsilyl Methacrylate and Poly-(dimethylsiloxane) Macromonomers Synthesized by RAFT Polymerization. *Polym. Chem.* **2013**, *4* (11), 3282−3292.
(19) Xu, W.; Ma, C.; Ma, J.; Gan, T.; Zhang, G. Marine Biofouling Resistance of Polyurethane with Biodegradation and Hydrolyzation. *ACS Appl. Mater. Interfaces* **2014**, *6* (6), 4017−4024.
(20) Jung, Y. S.; Ross, C. A. Orientation-Controlled Self-Assembled Nanolithography Using a Polystyrene−Polydimethylsiloxane Block Copolymer. *Nano Lett.* **2007**, *7* (7), 2046−2050.
(21) Andersen, T. H.; Tougaard, S.; Larsen, N. B.; Almdal, K.; Johannsen, I. Surface Morphology of PS−PDMS Diblock Copolymer Films. *J. Electron Spectrosc. Relat. Phenom.* **2001**, *121* (1−3), 93−110.
(22) Bakker, D. P.; Huijs, F. M.; de Vries, J.; Klijnstra, J. W.; Busscher, H. J.; van der Mei, H. C. Bacterial Deposition to Fluoridated and Non-Fluoridated Polyurethane Coatings with Different Elastic Modulus and Surface Tension in a Parallel Plate and a Stagnation Point Flow Chamber. *Colloids Surf., B* **2003**, *32* (3), 179−190.
(23) Ista, L. K.; Callow, M. E.; Finlay, J. A.; Coleman, S. E.; Nolasco, A. C.; Simons, R. H.; Callow, J. A.; Lopez, G. P. Effect of Substratum Surface Chemistry and Surface Energy on Attachment of Marine Bacteria and Algal Spores. *Appl. Environ. Microbiol.* **2004**, *70* (7), 4151−4157.
(24) Hahnel, S.; Rosentritt, M.; Handel, G.; Bürgers, R. Surface Characterization of Dental Ceramics and Initial Streptococcal Adhesion in Vitro. *Dent. Mater.* **2009**, *25* (8), 969−975.

DOI: 10.1021/acsami.5b04234
ACS Appl. Mater. Interfaces 2015, 7, 15578−15586